



1 **Response of dust emissions in southwestern North America to 21<sup>st</sup>**  
2 **century trends in climate, CO<sub>2</sub> fertilization, and land use:**  
3 **Implications for air quality**

4 Yang Li<sup>1</sup>, Loretta J. Mickley<sup>1</sup>, Jed O. Kaplan<sup>2</sup>

5 <sup>1</sup>John A. Paulson School of Engineering and Applied Sciences, Harvard University, Cambridge,  
6 MA, USA

7 <sup>2</sup>Department of Earth Sciences, The University of Hong Kong, Hong Kong, China

8 *Correspondence to:* Yang Li ([yangli@seas.harvard.edu](mailto:yangli@seas.harvard.edu))

9

10 **Abstract.** Climate models predict a shift toward warmer and drier environments in southwestern  
11 North America. However, the projected dust trends under climate change are sometimes  
12 contradictory. Here we link a dynamic vegetation model (LPJ-LMfire) to a chemical transport  
13 model (GEOS-Chem) to assess the impacts of future changes in climate, CO<sub>2</sub> fertilization, and  
14 land use practices on dust mobilization, and to investigate the consequences for surface air quality.  
15 Considering all factors in the most extreme future warming scenario, we find decreasing trends of  
16 fine dust emissions over Arizona and New Mexico but increasing emissions along Mexico's  
17 northern border in the late-21<sup>st</sup> century during springtime, the season of maximum dust emissions.  
18 These trends result from more densely vegetated environments in the arid southwestern U.S. under  
19 future climate, but sparser vegetation in northern Mexico. The two main drivers of dust trends in  
20 this region – CO<sub>2</sub> fertilization and land use intensification – play opposing roles, with the first  
21 driver enhancing vegetation and thus decreasing dust in the southwestern U.S. and the second  
22 driver increasing dust in northern Mexico. In the absence of CO<sub>2</sub> fertilization, the RCP8.5 scenario



23 places an upper bound on increases in dust, with elevated concentrations widespread over the  
24 southwestern North America by 2100 in spring, especially in southeastern New Mexico (up to ~2.0  
25  $\mu\text{g m}^{-3}$ ) and along the border between New Mexico and Mexico (up to ~2.5  $\mu\text{g m}^{-3}$ ).  
26



## 27 **1 Introduction**

28           Dust storms in the arid southwestern United States and northwestern Mexico (here defined  
29 as southwestern North America) entrain large quantities of soil-derived fine dust particles into the  
30 lower atmosphere and have negative effects on human health including causing respiratory and  
31 cardiovascular diseases (Tong et al., 2017; Meng and Lu, 2007; Gorris et al., 2018). Wind and  
32 vegetation cover are key factors that determine soil erodibility and dust emissions, with wind gusts  
33 mobilizing dust particles from the earth's surface and vegetation constraining dust emissions by  
34 reducing bare land and preserving soil moisture (Zender et al., 2003). A key question is to what  
35 extent climate change will influence future dust concentrations in the desert Southwest. While  
36 climate models predict a warmer and drier environment in this region through the 21<sup>st</sup> century  
37 (Seager and Vecchi, 2010), elevated CO<sub>2</sub> concentrations could enhance vegetation growth (Poorter  
38 and Perez-Soba, 2002). Land use practices in the future will likely also influence the propensity of  
39 dust storms. To investigate the potential effects of climate change, increasing CO<sub>2</sub> concentrations,  
40 and future land use practices on dust mobilization in southwestern North America, we couple a  
41 dynamic vegetation model (LPJ-LMfire) to a chemical transport model (GEOS-Chem) and  
42 perform a series of experiments in scenarios of future environmental conditions.

43           Previous studies investigated the relative importance of climate, CO<sub>2</sub> fertilization, and land  
44 use in present-day and future dust emissions and concentrations, sometimes with contradictory  
45 results. For example, Woodward et al., 2005 predicted a tripling of the global dust burden by 2100  
46 relative to the present day, while other studies suggested a decrease in the dust burden (e.g.,  
47 Harrison et al., 2001, Mahowald and Luo, 2003 and Mahowald et al., 2006). These estimates of  
48 future dust emissions depended in large part on the choice of model applied, as demonstrated by  
49 Tegen et al., 2004.



50 In southwestern North America, a few recent studies examined statistical relationships  
51 between observed present-day dust concentrations and meteorological conditions or leaf area index  
52 (LAI). Hand et al., 2016 found that fine dust concentrations in spring in this region correlated with  
53 the Pacific Decadal Oscillation (PDO), indicating the importance of large-scale climate patterns in  
54 the mobilization and transport of regional fine dust. Tong et al., 2017 further determined that the  
55 observed 240% increase in the frequency of windblown dust storms from 1990s to 2000s in the  
56 southwestern United States was likely associated with the PDO. Similarly, Achakulwisut et al.,  
57 2017 found that the 2002–2015 increase in average March fine dust concentrations in this region  
58 was driven by a combination of positive PDO conditions and phase of the El Niño-Southern  
59 Oscillation. More recently, Achakulwisut et al., 2018 identified the Precipitation-  
60 Evapotranspiration Index as a useful indicator of present-day dust variability. Applying that metric  
61 to an ensemble of future climate projections, these authors predicted increases of 26-46% in fine  
62 dust concentrations over the U.S. Southwest in spring by 2100. In contrast, Pu and Ginoux, 2017  
63 found that the frequency of extreme dust days decreases slightly in spring in this region due to  
64 reduced extent of bare land under 21<sup>st</sup> century climate change.

65 These previous studies relied mainly on statistical models that relate local and/or large  
66 scale meteorological conditions to dust emissions in southwestern North America. Pu and Ginoux,  
67 2017 also considered changing LAI in their model, but these dust-LAI relationships were derived  
68 from a relatively sparse dataset, casting some uncertainty on the results (Achakulwisut et al., 2018).  
69 In this study, we examine the response of dust mobilization due to climate-induced changes in  
70 vegetation, increasing CO<sub>2</sub> fertilization, and land use practices across the 21<sup>st</sup> century. We couple  
71 the LPJ-LMfire dynamic vegetation model to the chemical transport model GEOS-Chem to study  
72 vegetation dynamics and dust mobilization under different conditions and climate scenarios,



73 allowing consideration of many factors driving future dust mobilization in the southwestern North  
74 America. We focus on springtime (March, April, and May), because it is the season of highest dust  
75 concentrations in the southwestern U.S. (Hand et al., 2017).

76

## 77 **2 Methods**

78 We examine dust mobilization in southwestern North America, here defined as 25°N –  
79 37°N, 100°W – 115°W (Figure 1), during the late-21<sup>st</sup> century under future climate and land use  
80 based on two Representative Concentration Pathways (RCPs). RCP4.5 represents a moderate  
81 pathway with gradual reduction in greenhouse gas (GHG) emissions after 2050, while RCP8.5  
82 assumes continued increases in GHGs throughout the 21<sup>st</sup> century. To estimate changes in  
83 vegetation under future meteorological conditions, we use LPJ-LMfire, a dynamic global  
84 vegetation model that accounts for the effects of land use and fire on vegetation structure (Pfeiffer  
85 et al., 2013). Present-day and future meteorological fields, including surface temperature and  
86 precipitation, are simulated by the Goddard Institute for Space Studies (GISS) Model E climate  
87 model, and these are fed into LPJ-LMfire. For each RCP, we investigate the changes in vegetation  
88 following three scenarios: 1) an all-factor scenario that includes changes in climate, land use, and  
89 CO<sub>2</sub> fertilization; 2) a fixed-CO<sub>2</sub> scenario that includes changes in only climate and land use; and  
90 3) a fixed-land use scenario that includes changes in only climate and CO<sub>2</sub> fertilization. Using the  
91 GEOS-Chem emission component (HEMCO), we calculate dust emissions based on the LPJ-  
92 generated vegetation area index (VAI) in different scenarios. We then apply these dust emissions  
93 and the global chemical transport model GEOS-Chem to simulate the distribution of fine dust  
94 across the southwestern North America at a spatial resolution of 0.5° latitude x 0.625° longitude.  
95 For each RCP, the LPJ-LMfire simulation covers the period 2006-2100 continuously, with



96 monthly resolution. For computational reasons, we limit our GEOS-Chem simulations to two time-  
97 slices centered on the early and late 21<sup>st</sup> century, with each time slice covering 5 continuous years  
98 (2011-2015 and 2095-2099). We apply present-day meteorology to both time slices in GEOS-  
99 Chem, which allows us to focus on the effect of changing land cover on dust mobilization. More  
100 information is in the Methods section, including validation of the GEOS-Chem dust simulation for  
101 the present-day.

102 Under RCP4.5, the GISS model predicts a slight increase of 0.45 K in springtime mean  
103 surface temperatures and an increase in mean precipitation by ~17% over the southwestern North  
104 America by the 2100 time slice (2095-2099), relative to the present day (2011-2015). Under  
105 RCP8.5, the 5-year mean springtime temperature increases significantly by 3.29 K by 2100 and  
106 mean precipitation decreases by ~39%. The spatial distributions of the changes in temperature and  
107 precipitation by 2100 under RCP8.5 are presented in the Supplement (Figure S1).

## 108 **2.1 LPJ-LMfire**

109 LPJ-LMfire is driven by gridded climate, soil, land use fields, and atmospheric CO<sub>2</sub>  
110 concentrations, and simulates vegetation structure, biogeochemical cycling, and wildfire. The  
111 model takes into account the effects of fire activity on vegetation cover (Pfeiffer et al., 2013; Sitch  
112 et al., 2003). As described in Li et al., 2020, the model depends on a suite of meteorological  
113 anomalies from GISS-E2-R (Nazarenko et al., 2015) for RCP4.5 and RCP8.5: monthly mean  
114 surface temperature, diurnal temperature range, total monthly precipitation, number of days in the  
115 month with precipitation greater than 0.1 mm, monthly mean total cloud cover fraction, and  
116 monthly mean surface wind speed. Monthly mean lightning strike density, calculated using the  
117 GISS convective mass flux and the empirical parameterization of Magi, 2015, is also applied to  
118 LPJ-LMfire. Future land use scenarios applied follow CMIP5. In RCP8.5, the extent of cropland



119 and pasture cover increases by ~30% in Mexico but decreases by 10-20% over areas along  
120 Mexico's northern border in the U.S. (Hurtt et al., 2011). Minor changes in land use practices by  
121 2100 are predicted under RCP4.5 (Hurtt et al., 2011). We perform global simulations with LPJ-  
122 LMfire on a  $0.5^\circ \times 0.5^\circ$  grid for the two RCPs from 2006-2100, and analyze results over  
123 southwestern North America, where dust emissions are especially high.

124 Changes in climate, land use, and  $\text{CO}_2$  fertilization all play important roles in vegetation  
125 structure, which then in turn affects dust mobilization. RCP4.5 and RCP8.5 capture two possible  
126 climate trajectories over the 21<sup>st</sup> century, beginning in 2006. RCP4.5 represents a scenario of  
127 moderate future climate change with a radiative forcings at 2100 relative to pre-industrial values  
128 of  $+4.5 \text{ W m}^{-2}$ , while RCP8.5 represents a more extreme scenario with  $+8.5 \text{ W m}^{-2}$  at 2100. We  
129 probe the impacts of future meteorology on changes in vegetation type and vegetation density  
130 (vegetation area index, hereafter: VAI) using the LPJ-LMfire following three conditions: 1) the  
131 all-factor scenario which includes changes in climate, land use, and  $\text{CO}_2$  fertilization; 2) the fixed-  
132  $\text{CO}_2$  scenario which includes changes in only climate and land use; 3) the fixed-land use scenario  
133 which includes changes in only climate and  $\text{CO}_2$  fertilization. The GISS-E2-R meteorology used  
134 here covers the years 1801 to 2100 at a spatial resolution of  $2^\circ$  latitude  $\times$   $2.5^\circ$  longitude. To  
135 downscale the GISS meteorology to finer resolution for LPJ-LMfire, we calculate the 2010-2100  
136 monthly anomalies relative to the average over the 1961-1990 period, and then add these anomalies  
137 to an observationally based climatology at  $0.5^\circ$  latitude  $\times$   $0.5^\circ$  longitude (Pfeiffer et al., 2013).  
138 Compared to other climate models, the GISS model yields a conservative prediction of climate  
139 change in southwestern North America (Ahlström et al., 2012; Sheffield et al., 2013), which could  
140 result in conservative predictions of the impact of climate change on dust mobilization.

## 141 2.2 VAI calculation



142 Vegetation constrains dust emissions in two ways: 1) by competing with bare ground as a  
143 sink for atmospheric momentum, which results in less drag on erodible soil (Nicholson et al., 1998;  
144 Raupach, 1994); 2) and by enhancing soil moisture through plant shade and root systems (Hillel,  
145 1982). Here we implement the dust entrainment and deposition (DEAD) scheme of Zender et al.,  
146 2003 to compute a size-segregated dust flux, which includes entrainment thresholds for saltation,  
147 moisture inhibition, drag partitioning, and saltation feedback. It calculates the vertical dust flux as  
148 proportional to the horizontal saltation flux, and allows seasonally devegetated regions to mobilize  
149 dust. The DEAD dust scheme assumes that vegetation suppresses dust by linearly reducing  $A_m$ ,  
150 the fraction of bare soil exposed in each grid cell:

$$151 \quad A_m = (1 - A_l - A_w)(1 - A_s)(1 - A_v) \quad (1),$$

152 where  $A_l$  is the fraction of land covered by lakes,  $A_w$  is the fraction covered by wetlands,  $A_s$  is the  
153 fraction covered by snow, and  $A_v$  is the fraction covered by vegetation.

154 For this study, we use VAI as a metric to represent vegetation because it includes not only  
155 leaves but also stems and branches, all of which constrain dust emission. VAI is used to calculate  
156  $A_v$  in equation (1) through

$$157 \quad A_v = \min [1.0, \min(VAI, VAI_t) / VAI_t] \quad (2),$$

158 where  $VAI_t$  is the threshold as for complete suppression of dust emissions and is set as  $0.3 \text{ m}^2 \text{ m}^{-2}$   
159 (Zender et al., 2003; Mahowald et al., 1999).

160 LPJ-LMfire calculates the monthly leaf area indices (LAI) and fractional vegetation cover  
161 ( $\sigma_v$ ) for nine plant functional types (PFTs): tropical broadleaf evergreen, tropical broadleaf  
162 raingreen, temperate needleleaf evergreen, temperate broadleaf evergreen, temperate broadleaf  
163 summergreen, boreal needleleaf evergreen, and boreal summergreen trees, as well as  $C_3$  and  $C_4$   
164 grasses. Assuming immediate removal of all dead leaves as in Sellers et al., 1996,  $\sigma_v$  can be used



165 to represent stem area index (SAI) for different PFTs (Zeng et al., 2002). VAI is generally defined  
166 as the sum of the LAI plus SAI. As the threshold  $VAI_t$  for no dust emission is relatively low (i.e.,  
167  $0.3 \text{ m}^2 \text{ m}^{-2}$ ), leaf area has a dominant suppression effect on dust mobilization. In areas where LAI  
168 is greater than SAI, we assume that SAI does not play a role in controlling dust emissions and that  
169 LAI is equivalent to VAI. We also assume that  $C_3$  and  $C_4$  grasses have zero stem area to avoid  
170 overestimating VAI during the non-growing season when such grasses are dead. Based on the  
171 method of Zeng et al., 2002, with modifications, we calculate VAI in each grid cell as

$$172 \quad VAI = \max(\sum_{PFT=1}^9 LAI, \sum_{PFT=1}^7 \sigma_v) \quad (3)$$

173 where LAI and  $\sigma_v$  are from LPJ-LMfire.

### 174 **2.3 Calculation of dust emissions**

175 Dust emissions are calculated offline in the DEAD dust mobilization module within the  
176 Harvard-NASA Emissions Component (HEMCO). We feed into the DEAD module both the VAI  
177 generated by LPJ-LMfire and MERRA-2 meteorology at a spatial resolution of  $0.5^\circ$  latitude x  
178  $0.625^\circ$  longitude (Gelaro et al., 2017). Dust emission is nonlinear with surface windspeed.  
179 Following Ridley et al., 2013, we characterize subgrid-scale surface winds as a Weibull probability  
180 distribution, which allows dust saltation even when the grid-scale wind conditions are below some  
181 specified threshold speed. With this model setup, we calculate hourly dust emissions for two five-  
182 year time slices for each RCP and condition, covering the present day (2011-2015) and the late-  
183 21<sup>st</sup> century (2095-2099). Dust emissions are generated for four size bins with radii of  $0.1 - 1.0$   
184  $\mu\text{m}$ ,  $1.0 - 1.8 \mu\text{m}$ ,  $1.8 - 3.0 \mu\text{m}$ ,  $3.0 - 6.0 \mu\text{m}$ . These dust emissions are then applied to GEOS-  
185 Chem. Calculated present-day VAI and fine dust emissions are shown in Figure S2.

### 186 **2.4 GEOS-Chem**

187 We use the aerosol-only version of the GEOS-Chem chemical transport model (version



188 12.0.1; <http://acmg.seas.harvard.edu/geos/>). For computational efficiency, we apply monthly mean  
189 oxidants archived from a full-chemistry simulation (Park et al., 2004). To isolate the effect of  
190 changing dust mobilization on air quality over the southwestern North America, we use present-  
191 day MERRA-2 reanalysis meteorology from NASA/GMAO (Gelaro et al., 2017) for both the  
192 present-day and future time slices. In other words, we do not take into account changes in wind  
193 speeds in our simulations. For each time slice, we first carry out a global GEOS-Chem simulation  
194 at 4° latitude x 5° longitude spatial resolution, and then downscale to 0.5° x 0.625° via grid nesting  
195 over the North America domain. In this study, we focus only on dust particles in the finest size bin  
196 (i.e., with radii of 0.1 – 1.0 μm), as these are most deleterious to human health. We compare  
197 modeled fine dust concentrations over southwestern North America for the present-day against  
198 observations from the IMPROVE network in Figures S3-S4.

199

## 200 **3 Results**

### 201 **3.1 Spatial shifts in springtime vegetation area index**

202 Figure 1 shows large changes in the spatial distribution of modeled springtime VAI in the  
203 southwestern North America for the three scenarios under both RCPs by 2100. In RCP4.5, the  
204 distributions of changes in VAI are similar for the all-factor and fixed-land use scenarios. Strong  
205 enhancements (up to ~2.5 m<sup>2</sup> m<sup>-2</sup>) occur in the National Forests and Parks extending from the  
206 northwestern to southeastern corners of Arizona. The model exhibits moderate VAI increases in  
207 most of New Mexico and in the forest regions along the coast of northwestern Mexico. We find  
208 decreases in modeled VAI (up to ~ -1.6 m<sup>2</sup> m<sup>-2</sup>) in the southwestern corner of New Mexico, to the  
209 east of the coastal forests in Mexico and in the forest regions near the Mexican border connecting  
210 with southern Texas. The similarity between the two scenarios indicates the relatively trivial



211 influence of land use change on vegetation cover in RCP4.5. For the fixed-CO<sub>2</sub> scenario, western  
212 New Mexico and northern Mexico show greater decreases in VAI, indicating the role of CO<sub>2</sub>  
213 fertilization in balancing the effects of climate change on vegetation in this region. We also find  
214 scattered decreases in VAI in western Texas in this scenario. CO<sub>2</sub> fertilization has strong positive  
215 impacts on VAI (Figure S5).

216 Compared to RCP4.5, the RCP8.5 scenario shows larger changes in climate, CO<sub>2</sub>  
217 concentrations, and land use by 2100 (Figure 1). The net effects of these changes on vegetation  
218 are complex. As in RCP4.5, Arizona experiences a strong increase in VAI in the all-factor and  
219 fixed-land use scenarios, but now this increase extends to New Mexico. In contrast to RCP4.5,  
220 modeled VAI decreases in the coastal forest areas in northern Mexico in the all-factor RCP8.5  
221 scenario. In the fixed-land use scenario, however, the VAI decrease in northern Mexico is nearly  
222 erased, indicating the role of vegetation/forest degradation caused by land use practices (Figure  
223 S5). For the fixed-CO<sub>2</sub> scenario in RCP8.5, VAI decreases in nearly all of southwestern North  
224 America, except the northeastern corner of Arizona and the northwestern corner of New Mexico.

225 To better understand the changes in VAI, we can examine changes in LAI, which  
226 represents the major portion of VAI, for the four dominant plant functional types (PFTs) in this  
227 region. For example, decreases in LAI in the fixed-CO<sub>2</sub> scenario under RCP8.5 are dominated by  
228 the degradation of temperate broadleaf evergreen (TeBE) and temperate broadleaf summergreen  
229 (TeBS) (Figure S6). Temperate needleleaf evergreen (TeNE) shows areas of increase in the  
230 northern part and south of Texas in this scenario, while both TeBE and TeBS show increases in  
231 northern Arizona and New Mexico. In other areas, TeBS shows strong decreases, especially in  
232 southern Arizona and Mexico. C3 perennial grass (C3gr) makes only a minor contribution to the  
233 VAI decreases in this scenario, but this degradation plays an important role in dust mobilization.



234 As summarized in the Supplement (Figure S5), CO<sub>2</sub> fertilization and land use practices  
235 modify future vegetation cover in opposite ways. Under a warmer climate, higher CO<sub>2</sub>  
236 concentrations facilitate vegetation growth everywhere in the southwestern North America, with  
237 larger VAI increases occurring over Arizona and New Mexico. Projected land use practices –  
238 which include agriculture, human settlement, and urban sprawl – result in habitat loss and the  
239 fragmentation of forested landscapes. These trends in land use decrease VAI, especially in RCP8.5  
240 in the coastal forest regions of Mexico and along the northeastern border of Mexico south of Texas.

### 241 **3.2 Spatial variations in spring fine dust emissions**

242 Unlike the widespread changes in VAI, future changes in fine dust emissions are  
243 concentrated in a few arid areas, including: 1) the border regions connecting Arizona, New Mexico,  
244 and northern Mexico (ANM border), 2) eastern New Mexico, and 3) western Texas (Figure 2). In  
245 RCP4.5, slight increases in fine dust emission (up to ~0.3 kg m<sup>-2</sup> mon<sup>-1</sup>) are simulated in the ANM  
246 border in all the three scenarios, indicating desertification of the southern semi-arid highlands  
247 between the Sonoran and Chihuahuan deserts. In contrast, fine dust emissions decrease by up to ~  
248 -1.0 kg m<sup>-2</sup> mon<sup>-1</sup> in eastern New Mexico and western Texas in RCP4.5 due to warmer  
249 temperatures and increasing VAI. Consistent with the modest changes in VAI (Figure 1), the three  
250 scenarios in RCP4.5 do not exhibit large differences, with only the fixed-CO<sub>2</sub> scenario showing  
251 slightly greater increases in dust emissions along the ANM border and in western Texas. In RCP8.5  
252 in the all-factor scenario, spring fine dust emissions increase slightly by up to ~ 0.4 kg m<sup>-2</sup> mon<sup>-1</sup>  
253 along the ANM border, but decrease more strongly in western Texas by up to ~ -1.4 kg m<sup>-2</sup> mon<sup>-1</sup>  
254 (Figure 2). In contrast, with fixed CO<sub>2</sub> the sign of the change in dust emissions reverses, with  
255 significant emissions increases along the ANM border and in New Mexico. The area with  
256 decreasing emissions in western Texas also shrinks in this scenario. These trends occur due to the



257 climate stresses on temperature broadleaf trees and C3 grasses that are not counteracted in this  
258 scenario by CO<sub>2</sub> fertilization (Figure S5).

259 Figure 3 shows more vividly the opposing roles of CO<sub>2</sub> fertilization and projected land use  
260 change in southwestern North America. In RCP8.5, changing CO<sub>2</sub> fertilization alone promotes  
261 vegetation growth and dramatically reduces dust mobilization by up to  $\sim -1.2 \text{ kg m}^{-2} \text{ mon}^{-1}$ . Figure  
262 3 also shows that land use trends are a major driver of dust emissions along the ANM border and  
263 western Texas. Again in RCP8.5, the land use scenario shows abandonment of crop- and  
264 rangelands in this region, curtailing dust emissions (Hurt et al., 2011). However, the projection of  
265 rangeland expansion in northern Mexico in RCP8.5 reduces natural vegetation cover in this region  
266 (Hurt et al., 2011), contributing to the increase of fine dust emissions by up to  $\sim 0.7 \text{ kg m}^{-2} \text{ mon}^{-1}$ .

### 267 **3.3 Spring fine dust concentrations under the high emission scenario**

268 Our simulations suggest that fine dust emissions will increase across arid areas in  
269 southwestern North America under RCP8.5, but only if CO<sub>2</sub> fertilization is of minimal importance  
270 (Figure 2). To place an upper bound on future concentrations of fine dust in this region, we apply  
271 only the fixed-CO<sub>2</sub> emissions to GEOS-Chem at the horizontal resolution of  $0.5^\circ \times 0.625^\circ$ . Given  
272 the large uncertainty in the sensitivity of vegetation to changing atmospheric CO<sub>2</sub> concentrations  
273 (Smith et al., 2016), we argue that this approach is justified.

274 Results from GEOS-Chem show that the concentrations of spring fine dust are significantly  
275 enhanced in the southeastern half of New Mexico and along the ANM border, with increases up  
276 to  $\sim 2.5 \mu\text{g m}^{-3}$  (Figure 4). The model also yields elevated dust concentrations over nearly the entire  
277 extent of our study region by 2100. While anthropogenic land use serves as a major driver of the  
278 dust increases along the ANM border, climate change accounts for the bulk of these increases,  
279 with winds transporting the enhanced dust across much of the region. We find that dust decreases



280 in this scenario only in a limited area in western Texas due to changing land use (Figure 3).

281

#### 282 **4 Discussion**

283 We apply a coupled modeling approach to investigate the impact of future changes in  
284 climate, CO<sub>2</sub> fertilization, and anthropogenic land use on dust mobilization and dust concentration  
285 in southwestern North America by the end of the 21<sup>st</sup> century. Table 1 summarizes our findings  
286 for the two RCP scenarios and three conditions – all-factor, fixed CO<sub>2</sub>, and fixed land use – in  
287 spring, when dust concentrations are greatest.

288 We find that in the RCP8.5 fixed-CO<sub>2</sub> scenario, in which the effects of CO<sub>2</sub> fertilization  
289 are neglected, VAI decreases by 26% across the region due to warmer temperatures and drier  
290 conditions, yielding an increase of 58% in fine dust emission averaged over the southwestern North  
291 America. Specifically, the increase in fine dust emission in northern Mexico is mainly driven by  
292 the increases in the extent of cropland and pasture cover in this area, signifying the crucial role of  
293 land use practices in modifying dust mobilization. The 58% increase predicted in this study is  
294 larger than the 26-46% future increases in fine dust for this region predicted by the statistical model  
295 of Achakulwisut et al., 2018. In contrast, the statistical model of Pu and Ginoux, 2017 estimated  
296 a decrease by ~2% in the springtime frequency of extreme dust events in the Southwest U.S.,  
297 driven by reductions in bare ground fraction and wind speed. Differences between our study and  
298 these two previous ones highlight the importance of robust representation of both future vegetation  
299 changes and the sensitivity of dust emissions to these changes. The study of Achakulwisut et al.,  
300 2018 did not consider the climate effect on vegetation, while that of Pu and Ginoux, 2017 relied  
301 on limited data for capturing the sensitivity of dust to land cover in this region. Neither study  
302 considered changes in land use.



303 We further find that consideration of CO<sub>2</sub> fertilization can mitigate the effects of changing  
304 climate and land use on dust concentrations in southwestern North America. The all-factor and  
305 fixed-land use simulations both yield decreases of ~20% in mean dust emissions compared to the  
306 early 21<sup>st</sup> century. In the IPCC projections, CO<sub>2</sub> reaches ~550 ppm by 2100 under RCP4.5 and  
307 ~1960 ppm under RCP8.5 (Meinshausen et al., 2011). Correspondingly, CO<sub>2</sub> fertilization enhances  
308 VAI by 30% by 2100 under RCP4.5 and 64% under RCP8.5. These enhancements further decrease  
309 fine dust emissions by 21% under RCP4.5 and 78% under RCP8.5, compared to the present day.  
310 Except along the ANM border and a few other areas, trends in land use have only minor impacts  
311 on dust mobilization under the two RCPs in southwestern North America.

312 Our study suggests that CO<sub>2</sub> fertilization plays a major role in modifying vegetation cover  
313 and, in some regions, reverses the sign of future dust emission trends from positive to negative by  
314 2100. However, there is large uncertainty in quantifying the sensitivity of vegetation to ambient  
315 CO<sub>2</sub>, with at least one study suggesting that models may overestimate this sensitivity (Smith et al.,  
316 2016). One reason for this uncertainty is incomplete understanding of the nutrient constraints on  
317 plant growth (Wieder et al., 2015), which vary greatly among different PFTs (Shaw et al., 2002;  
318 Nadelhoffer et al., 1999). Additionally, understanding the drivers in historic dust trends has  
319 sometimes been challenging (Mahowald and Luo, 2003; Mahowald et al., 2002), making it  
320 difficult to validate dust mobilization models. A further drawback of our approach is that the LPJ-  
321 LMfire model is driven by meteorological fields from just one climate model, GISS-E2-R. Given  
322 that the GISS model yields a conservative prediction of climate change in the southwestern North  
323 America compared to other models (Ahlström et al., 2012; Sheffield et al., 2013), our predictions  
324 of the impact of climate change on dust mobilization may also be conservative. Finally, our study



325 focuses only on the effect of changing vegetation on dust mobilization and does not take into  
326 account how changing windspeeds may also influence dust.

327 Within these limitations, our study quantifies the potential impacts of climate change and land  
328 use practices on dust mobilization over the coming decades. For example, if the effects of CO<sub>2</sub>  
329 fertilization on vegetation growth are attenuated by nutrient constraints, our work suggests a  
330 potentially large climate penalty on air quality, with consequences for human health by 2100 across  
331 much of southwestern North America.

332

### 333 **Code and data availability**

334 GEOS-Chem model codes can be obtained at <http://acmg.seas.harvard.edu/geos>. LPJ-LMfire  
335 model codes can be obtained at <https://github.com/ARVE-Research/LPJ-LMfire>. IMPROVE  
336 datasets are available online at <http://vista.cira.colostate.edu/improve>. Any additional information  
337 related to this paper may be requested from the authors.

338

### 339 **Author contributions**

340 Y.L. conceived and designed the study, performed the GEOS-Chem simulations, analyzed the data,  
341 and wrote the manuscript, with contributions from all coauthors. J.O.K. performed the LPJ-LMfire  
342 simulations.

343

### 344 **Competing interests**

345 The authors declare that they have no competing interest.

346



347 **Acknowledgments**

348 This research was developed under Assistance Agreements 83587501 and 83587201 awarded by  
349 the U.S. Environmental Protection Agency (EPA). It has not been formally reviewed by the EPA.  
350 The views expressed in this document are solely those of the authors and do not necessarily reflect  
351 those of the EPA. We thank all of the data providers of the datasets used in this study. PM data  
352 was provided by the Interagency Monitoring of Protected Visual Environments (IMPROVE;  
353 available online at <http://vista.cira.colostate.edu/improve>). IMPROVE is a collaborative  
354 association of state, tribal, and federal agencies, and international partners. U.S. Environmental  
355 Protection Agency is the primary funding source, with contracting and research support from the  
356 National Park Service. JOK is grateful for access to computing resources provided by the School  
357 of Geography and the Environment, University of Oxford. The Air Quality Group at the University  
358 of California, Davis is the central analytical laboratory, with ion analysis provided by the Research  
359 Triangle Institute, and carbon analysis provided by the Desert Research Institute. We acknowledge  
360 the World Climate Research Programme's Working Group on Coupled Modelling, which is  
361 responsible for CMIP, and we thank the group of NASA Goddard Institute for Space Studies for  
362 producing and making available their GISS-E2-R climate model output. For CMIP the U.S.  
363 Department of Energy's Program for Climate Model Diagnosis and Intercomparison provides  
364 coordinating support and led development of software infrastructure in partnership with the Global  
365 Organization for Earth System Science Portals. The GISS-E2-R dataset were downloaded from  
366 <https://cmip.llnl.gov/cmip5/>. We thank the Land-use Harmonization team for producing the  
367 harmonized set of land-use scenarios and making available the dataset online at  
368 <http://tntcat.iiasa.ac.at/RcpDb/>.

369



## 370 References

- 371 Achakulwisut, P., Shen, L., and Mickley, L. J.: What controls springtime fine dust variability in  
372 the western United States? Investigating the 2002–2015 increase in fine dust in the US  
373 Southwest, *Journal of Geophysical Research: Atmospheres*, 122, 2017.
- 374 Achakulwisut, P., Mickley, L., and Anenberg, S.: Drought-sensitivity of fine dust in the US  
375 Southwest: Implications for air quality and public health under future climate change,  
376 *Environmental Research Letters*, 13, 054025, 2018.
- 377 Ahlström, A., Schurgers, G., Arneth, A., and Smith, B.: Robustness and uncertainty in terrestrial  
378 ecosystem carbon response to CMIP5 climate change projections, *Environmental Research  
379 Letters*, 7, 044008, 2012.
- 380 Gelaro, R., McCarty, W., Suárez, M. J., Todling, R., Molod, A., Takacs, L., Randles, C. A.,  
381 Darmenov, A., Bosilovich, M. G., and Reichle, R.: The modern-era retrospective analysis for  
382 research and applications, version 2 (MERRA-2), *Journal of Climate*, 30, 5419–5454, 2017.
- 383 Gorris, M., Cat, L., Zender, C., Treseder, K., and Randerson, J.: Coccidioidomycosis dynamics  
384 in relation to climate in the southwestern United States, *GeoHealth*, 2, 6–24, 2018.
- 385 Hand, J., White, W., Gebhart, K., Hyslop, N., Gill, T., and Schichtel, B.: Earlier onset of the  
386 spring fine dust season in the southwestern United States, *Geophysical Research Letters*, 43,  
387 4001–4009, 2016.
- 388 Hand, J., Gill, T., and Schichtel, B.: Spatial and seasonal variability in fine mineral dust and  
389 coarse aerosol mass at remote sites across the United States, *Journal of Geophysical Research:  
390 Atmospheres*, 122, 3080–3097, 2017.
- 391 Harrison, S. P., Kohfeld, K. E., Roelandt, C., and Claquin, T.: The role of dust in climate  
392 changes today, at the last glacial maximum and in the future, *Earth-Science Reviews*, 54, 43–  
393 80, 2001.
- 394 Hillel, D.: *Introduction to soil physics.* (Academic Press: San Diego, CA), *Introduction to soil  
395 physics.* Academic Press, San Diego, CA., -, 1982.
- 396 Hurr, G. C., Chini, L. P., Frolking, S., Betts, R., Feddema, J., Fischer, G., Fisk, J., Hibbard, K.,  
397 Houghton, R., and Janetos, A.: Harmonization of land-use scenarios for the period 1500–  
398 2100: 600 years of global gridded annual land-use transitions, wood harvest, and resulting  
399 secondary lands, *Climatic change*, 109, 117, 2011.
- 400 Li, Y., Mickley, L. J., Liu, P., and Kaplan, J. O.: Trends and spatial shifts in lightning fires and  
401 smoke concentrations in response to 21st century climate over the forests of the Western  
402 United States, *Atmos. Chem. Phys. Discuss.*, 2020, 1–26, 10.5194/acp-2020-80, 2020.
- 403 Magi, B. I.: Global lightning parameterization from CMIP5 climate model output, *Journal of  
404 Atmospheric and Oceanic Technology*, 32, 434–452, 2015.
- 405 Mahowald, N., Kohfeld, K., Hansson, M., Balkanski, Y., Harrison, S. P., Prentice, I. C., Schulz,  
406 M., and Rodhe, H.: Dust sources and deposition during the last glacial maximum and current  
407 climate: A comparison of model results with paleodata from ice cores and marine sediments,  
408 *Journal of Geophysical Research: Atmospheres*, 104, 15895–15916, 1999.
- 409 Mahowald, N. M., Zender, C. S., Luo, C., Savoie, D., Torres, O., and Del Corral, J.:  
410 Understanding the 30-year Barbados desert dust record, *Journal of Geophysical Research:  
411 Atmospheres*, 107, AAC 7-1–AAC 7-16, 2002.
- 412 Mahowald, N. M., and Luo, C.: A less dusty future?, *Geophysical Research Letters*, 30, 2003.
- 413 Mahowald, N. M., Muhs, D. R., Levis, S., Rasch, P. J., Yoshioka, M., Zender, C. S., and Luo, C.:  
414 Change in atmospheric mineral aerosols in response to climate: Last glacial period,



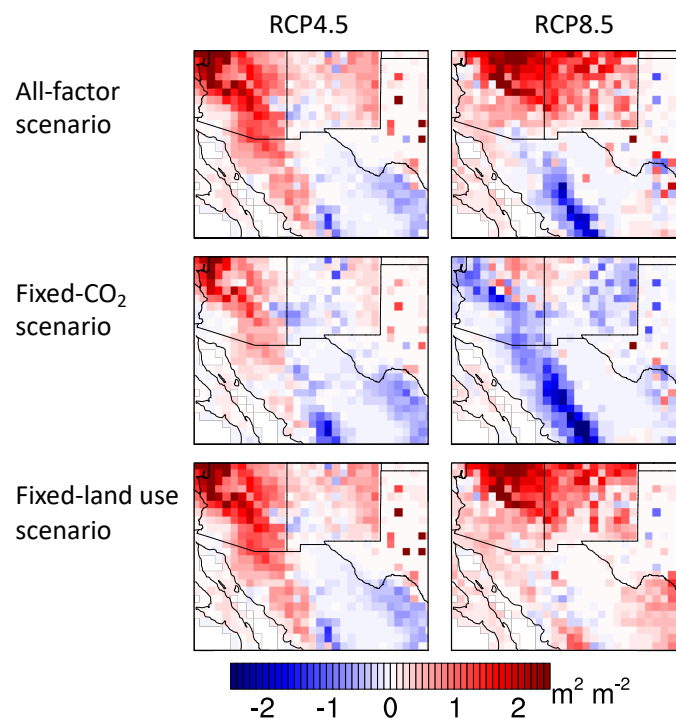
- 415 preindustrial, modern, and doubled carbon dioxide climates, *Journal of Geophysical Research:*  
416 *Atmospheres*, 111, 2006.
- 417 Meinshausen, M., Smith, S. J., Calvin, K., Daniel, J. S., Kainuma, M., Lamarque, J.-F.,  
418 Matsumoto, K., Montzka, S., Raper, S., and Riahi, K.: The RCP greenhouse gas  
419 concentrations and their extensions from 1765 to 2300, *Climatic change*, 109, 213, 2011.
- 420 Meng, Z., and Lu, B.: Dust events as a risk factor for daily hospitalization for respiratory and  
421 cardiovascular diseases in Minqin, China, *Atmos Environ*, 41, 7048-7058, 2007.
- 422 Nadelhoffer, K. J., Emmett, B. A., Gundersen, P., Kjønaas, O. J., Koopmans, C. J., Schleppi, P.,  
423 Tietema, A., and Wright, R. F.: Nitrogen deposition makes a minor contribution to carbon  
424 sequestration in temperate forests, *Nature*, 398, 145, 1999.
- 425 Nazarenko, L., Schmidt, G., Miller, R., Tausnev, N., Kelley, M., Ruedy, R., Russell, G., Aleinov,  
426 I., Bauer, M., and Bauer, S.: Future climate change under RCP emission scenarios with GISS  
427 ModelE2, *Journal of Advances in Modeling Earth Systems*, 7, 244-267, 2015.
- 428 Nicholson, S. E., Tucker, C. J., and Ba, M.: Desertification, drought, and surface vegetation: An  
429 example from the West African Sahel, *Bulletin of the American Meteorological Society*, 79,  
430 815-830, 1998.
- 431 Park, R. J., Jacob, D. J., Field, B. D., Yantosca, R. M., and Chin, M.: Natural and transboundary  
432 pollution influences on sulfate-nitrate-ammonium aerosols in the United States: Implications  
433 for policy, *Journal of Geophysical Research: Atmospheres*, 109, 2004.
- 434 Pfeiffer, M., Spessa, A., and Kaplan, J. O.: A model for global biomass burning in preindustrial  
435 time: LPJ-LMfire (v1. 0), *Geoscientific Model Development*, 6, 643-685, 2013.
- 436 Poorter, H., and Perez-Soba, M.: Plant growth at elevated CO<sub>2</sub>, *Encyclopedia of global  
437 environmental change*, 2, 489-496, 2002.
- 438 Pu, B., and Ginoux, P.: Projection of American dustiness in the late 21<sup>st</sup> century due to climate  
439 change, *Scientific reports*, 7, 5553, 2017.
- 440 Raupach, M.: Simplified expressions for vegetation roughness length and zero-plane  
441 displacement as functions of canopy height and area index, *Boundary-Layer Meteorol*, 71,  
442 211-216, 1994.
- 443 Ridley, D. A., Heald, C. L., Pierce, J., and Evans, M.: Toward resolution-independent dust  
444 emissions in global models: Impacts on the seasonal and spatial distribution of dust,  
445 *Geophysical Research Letters*, 40, 2873-2877, 2013.
- 446 Seager, R., and Vecchi, G. A.: Greenhouse warming and the 21<sup>st</sup> century hydroclimate of  
447 southwestern North America, *Proceedings of the National Academy of Sciences*, 107, 21277-  
448 21282, 2010.
- 449 Sellers, P. J., Tucker, C. J., Collatz, G. J., Los, S. O., Justice, C. O., Dazlich, D. A., and Randall,  
450 D. A.: A revised land surface parameterization (SiB2) for atmospheric GCMs. Part II: The  
451 generation of global fields of terrestrial biophysical parameters from satellite data, *Journal of  
452 climate*, 9, 706-737, 1996.
- 453 Shaw, M. R., Zavaleta, E. S., Chiariello, N. R., Cleland, E. E., Mooney, H. A., and Field, C. B.:  
454 Grassland responses to global environmental changes suppressed by elevated CO<sub>2</sub>, *science*,  
455 298, 1987-1990, 2002.
- 456 Sheffield, J., Barrett, A. P., Colle, B., Nelun Fernando, D., Fu, R., Geil, K. L., Hu, Q., Kinter, J.,  
457 Kumar, S., and Langenbrunner, B.: North American climate in CMIP5 experiments. Part I:  
458 Evaluation of historical simulations of continental and regional climatology, *Journal of  
459 Climate*, 26, 9209-9245, 2013.



- 460 Sitch, S., Smith, B., Prentice, I. C., Arneeth, A., Bondeau, A., Cramer, W., Kaplan, J. O., Levis,  
461 S., Lucht, W., and Sykes, M. T.: Evaluation of ecosystem dynamics, plant geography and  
462 terrestrial carbon cycling in the LPJ dynamic global vegetation model, *Global Change*  
463 *Biology*, 9, 161-185, 2003.
- 464 Smith, W. K., Reed, S. C., Cleveland, C. C., Ballantyne, A. P., Anderegg, W. R., Wieder, W. R.,  
465 Liu, Y. Y., and Running, S. W.: Large divergence of satellite and Earth system model  
466 estimates of global terrestrial CO<sub>2</sub> fertilization, *Nature Climate Change*, 6, 306, 2016.
- 467 Tegen, I., Werner, M., Harrison, S., and Kohfeld, K.: Relative importance of climate and land  
468 use in determining present and future global soil dust emission, *Geophysical Research Letters*,  
469 31, 2004.
- 470 Tong, D. Q., Wang, J. X., Gill, T. E., Lei, H., and Wang, B.: Intensified dust storm activity and  
471 Valley fever infection in the southwestern United States, *Geophysical research letters*, 44,  
472 4304-4312, 2017.
- 473 Wieder, W. R., Cleveland, C. C., Smith, W. K., and Todd-Brown, K.: Future productivity and  
474 carbon storage limited by terrestrial nutrient availability, *Nature Geoscience*, 8, 441, 2015.
- 475 Woodward, S., Roberts, D., and Betts, R.: A simulation of the effect of climate change-induced  
476 desertification on mineral dust aerosol, *Geophysical Research Letters*, 32, 2005.
- 477 Zender, C. S., Bian, H., and Newman, D.: Mineral Dust Entrainment and Deposition (DEAD)  
478 model: Description and 1990s dust climatology, *Journal of Geophysical Research:*  
479 *Atmospheres*, 108, 2003.
- 480 Zeng, X., Shaikh, M., Dai, Y., Dickinson, R. E., and Myneni, R.: Coupling of the common land  
481 model to the NCAR community climate model, *Journal of Climate*, 15, 1832-1854, 2002.
- 482
- 483



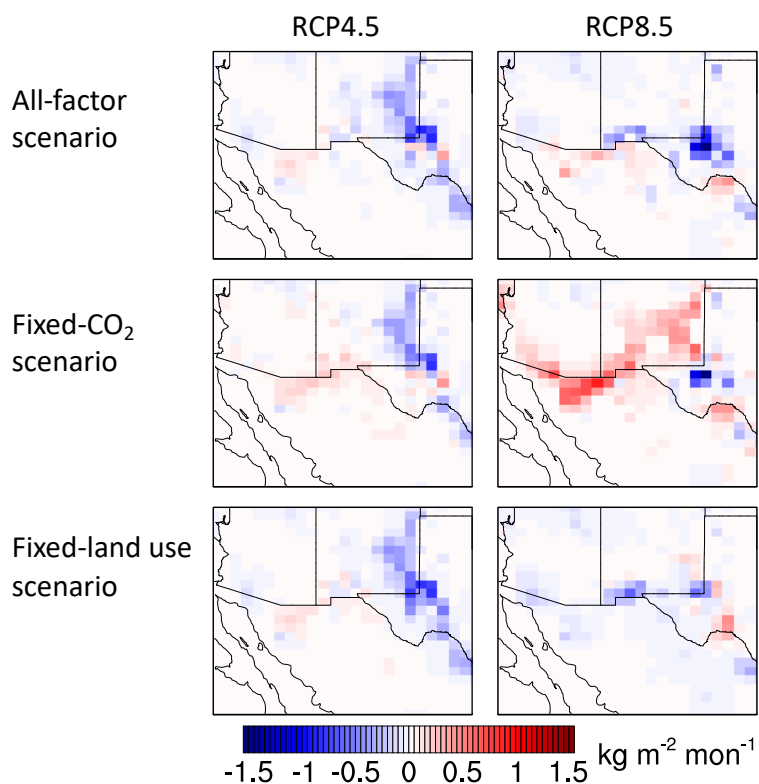
484 **Figures and tables**



485

486 **Figure 1.** Simulated changes in spring averaged monthly mean vegetation area index (VAI) in  
487 southwestern North America under the three conditions for RCP4.5 and RCP8.5. Changes are  
488 between the present day and 2100, with five years representing each time period. The All-factor  
489 scenario (top row) includes the effects of climate, CO<sub>2</sub> fertilization, and anthropogenic land use on  
490 vegetation. Only climate and land use are considered in the Fixed-CO<sub>2</sub> scenario (middle), and only  
491 climate and CO<sub>2</sub> fertilization are considered in the Fixed-land use scenario (bottom). Results are  
492 from LPJ-LMfire.

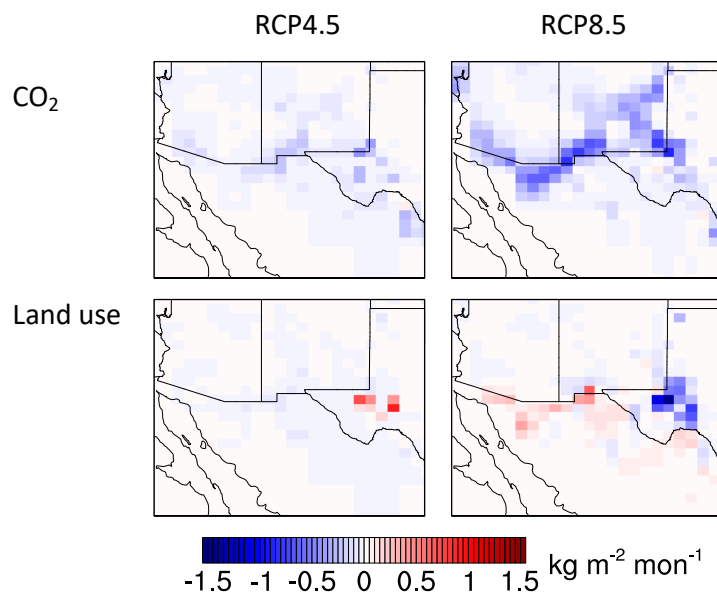
493



494

495 **Figure 2.** Simulated changes in spring averaged monthly mean dust emission in southwestern  
496 North America under the three conditions for RCP4.5 and RCP8.5. Changes are between the  
497 present day and 2100, with five years representing each time period. The top row shows results for  
498 the all-factor condition, the middle row is for the fixed-CO<sub>2</sub> condition, and the bottom row is for  
499 the fixed-land use condition. Scenarios are described in Figure 1. Results are generated offline  
500 using the GEOS-Chem emission component (HEMCO).

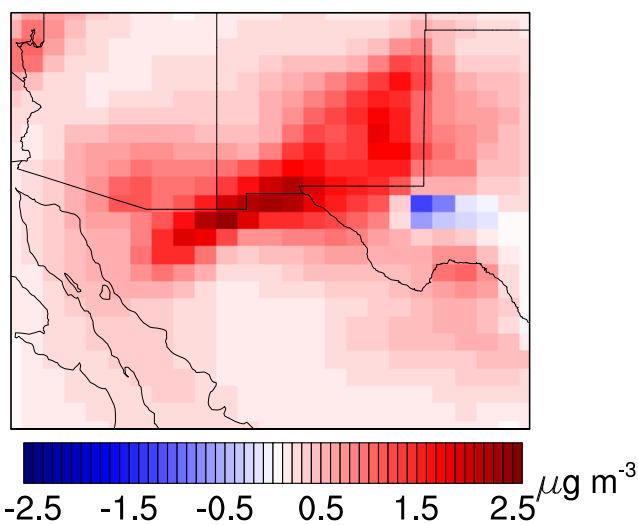
501



502

503 **Figure 3.** Contributions of CO<sub>2</sub> fertilization and land use change to changing dust emissions in  
504 spring in southwestern North America for RCP4.5 and RCP8.5. Changes are between the present  
505 day and 2100, with five years representing each time period. The top row shows the response of  
506 dust emission to only CO<sub>2</sub> fertilization and the bottom row shows the response to only trends in  
507 land use. Results are generated offline using the GEOS-Chem emission component (HEMCO).

508



509

510 **Figure 4.** Simulated changes in springtime mean concentrations of fine dust over southwestern  
511 North America for the RCP8.5 fixed-CO<sub>2</sub> scenario, in which the effects of CO<sub>2</sub> fertilization are  
512 neglected. Changes are between the present day and 2100, with five years representing each time  
513 period. Results are from GEOS-Chem simulations at 0.5° x 0.625° resolution.

514



515 **Table 1.** Averaged spring vegetation area index (VAI) and fine dust emission in southwestern  
 516 North America for the present-day and future for two scenarios (RCP4.5 and RCP8.5) and three  
 517 cases. The all-factor case includes changes in climate, land use, and CO<sub>2</sub> fertilization; the fixed-  
 518 CO<sub>2</sub> case includes changes in only climate and land use; and the fixed-land use case includes  
 519 changes in only climate and CO<sub>2</sub>.

		VAI <sup>b</sup> , m <sup>2</sup> m <sup>-2</sup>			Fine dust emission <sup>b</sup> , kg m <sup>-2</sup> mon <sup>-1</sup>		
		All-factor	Fixed CO <sub>2</sub>	Fixed land use	All-factor	Fixed CO <sub>2</sub>	Fixed land use
<b>RCP4.5</b>	<b>2010<sup>a</sup></b>	0.75±0.26	0.71±0.24	0.75±0.26	0.10±0.07	0.11±0.08	0.10±0.07
	<b>2100<sup>a</sup></b>	1.07±0.48	0.79±0.34	1.07±0.48	0.08±0.04	0.10±0.05	0.08±0.04
<b>2100-2010, %</b>		<b>42</b>	<b>12</b>	<b>42</b>	<b>-25</b>	<b>-4</b>	<b>-26</b>
<b>RCP8.5</b>	<b>2010<sup>a</sup></b>	0.80±0.27	0.75±0.24	0.75±0.24	0.09±0.04	0.09±0.05	0.09±0.04
	<b>2100<sup>a</sup></b>	1.11±0.71	0.55±0.33	0.55±0.33	0.07±0.04	0.14±0.09	0.07±0.06
<b>2100-2010, %</b>		<b>38</b>	<b>-26</b>	<b>52</b>	<b>-20</b>	<b>58</b>	<b>-16</b>

520 <sup>a</sup>Each time slice represents 5 years; <sup>b</sup>Values are spring (MAM) averages over southwestern North America.